Available online at www.sciencedirect.com
ScienceDirect
International Journal of Thermal Sciences 46 (2007) 319–327
International Journal of Thermal Sciences
www.elsevier.com/locate/ijts

Modelling thermal degradation of woody fuel particles

B. Benkoussas [a], J.-L. Consalvi [b,*], B. Porterie [b], N. Sardoy [b], J.-C. Loraud [b]

[a] *Ecole Nationale Polytechnique, 10 avenue Hassen Badi El-Harrach, Alger, Algeria*
[b] *IUSTI/UMR CNRS 6595, 5 rue E. Fermi, 13453 Marseille Cedex 13, France*

Received 1 August 2005; received in revised form 20 June 2006; accepted 30 June 2006

Available online 23 October 2006

Abstract

A model for thermal degradation of woody fuel particles is developed. It includes drying, pyrolysis, and char oxidation processes. The model is first applied to assess the validity of the thermally-thin pyrolysis assumption commonly used in wildfire behavior models. For a given external radiant heat flux, the particle size at which transition between thermally-thin and thermally-thick pyrolysis regimes occurs is evaluated by comparing the pyrolysis times computed for both regimes. It is found that, for a given flux, the particle size above which the thermally-thin assumption is questionable, is independent on the moisture content and on the particle surface-area-to-volume ratio. This means that the transition characteristic lengths for spheres, cylinders and slabs are related by: $L_{cr} = L_{cr,slab} = L_{cr,cyl}/2 = L_{cr,sph}/3$. A Biot number based on the particle surface-area-to-volume ratio, σ_p can then be defined as $Bi = \varepsilon_w Q_{ext}/\lambda_w \sigma_p \Delta T$. Results show that the thermally-thin regime can be defined by $Bi < 0.1$ whatever the particle shape. They reveal that the traditional thermally-thin pyrolysis assumption is not suitable to model wildland fire behavior. For thin particles responsible for fire spread pyrolysis is kinetically-controlled while it is controlled by heat diffusion for large particles. Secondly, the model is applied to the combustion of firebrands. Model results are found in good agreement with available experimental data.

Keywords: Thermal degradation; Wildland fuels; Pyrolysis; Biot number; Firebrands

1. Introduction

Wildland fire spread depends mainly on the heat transfer from the flame and burning region of the fuel bed to the unburnt solid material, which in turn decomposes into volatile gases. These pyrolysis products convect and diffuse outwards, and mix with air to form a combustible mixture ahead of the flame leading edge. Then this mixture is ignited by the flame. Thermal degradation process can be divided into three stages: drying, pyrolysis, and char oxidation. As a consequence of wildland fuel pyrolysis, after drying, combustible and non combustible gases, char, and soot are formed. For forest fuel matter, char consists of pure carbon (80–97%) and ash. If oxygen is present at the surface of the incandescent charreous particles and temperature is high enough, an exothermic heterogeneous global char oxidation takes place.

The modelling of thermal degradation is complex because of the strong coupling between chemical and heat and mass transfer processes. It is a well established fact that the spread rate of wildland fires is often determined by burning in fine fuels [1]. As a result, most theoretical studies on wildfire propagation were conducted assuming thermally-thin fuel particles [2,3]. The range of validity of this assumption depends widely on the particle size and on the amount of heat transferred from the flame to the unburnt fuel. Moreover, larger fuel particles contribute to the fire intensity and flaming zone combustion as well as the fuel consumption ratio [1]. On another hand, previous analysis [4] have shown that firebrands responsible for spotting are thermally-thick particles. Spotting is the process whereby flaming or glowing firebrands are transported ahead of the source fire to initiate new fires called spot fires [4]. The firebrands may be transported by wind alone or be initially lofted by a convection column, fire plume or fire whirl [5,6]. The probability of fuel bed ignition by flaming firebrands has been modelled [7]. The capability of a firebrand to initiate a new spot fire depends mainly on its energetic content at landing.

* Corresponding author. Tel.: (+33) 491 106 927; fax: (+33) 491 106 969.
E-mail address: jean-louis.consalvi@polytech.univ-mrs.fr (J.-L. Consalvi).

1290-0729/$ – see front matter
doi:10.1016/j.ijthermalsci.2006.06.016

Nomenclature

C_p	specific heat
h	heat transfer coefficient
L_v	latent heat of vaporization
L_{char}	heat of char oxidation
m''	mass flux
M	moisture
Q_{ext}	external heat flux
R	particle radius
r	radial distance
R_{H_2O}	rate of vaporization
R_{pyr}	rate of pyrolysis
R_{char}	rate of char oxidation
Re	Reynolds number
Sc	Schmidt number
S_p	particle surface
V_p	particle volume
Y_{O_2}	oxygen mass fraction in the oxidant gas flow
ΔH_{pyr}	heat of pyrolysis

Greek symbols

ρ	density
σ_p	particle surface-area-to-volume ratio
ν_{char}	char mass fraction
χ	specific gravity
ε	surface emissivity
α	thermal diffusivity

Subscripts and superscripts

amb	ambient
cr	transition
conv	convection
m	moisture
pyr	pyrolysis
w	wood
w_0	dry wood

The aim of this paper is to propose a simplified thermally-thick model including the main chemical processes occurring during thermal degradation of wildland fuel particles, namely drying, pyrolysis, and char combustion. This model is first applied to explore the suitability of the thermally-thin assumption to describe the pyrolysis of vegetal particles. Second, this model is applied to the combustion of firebrands and comparisons with experiments are performed.

2. Previous studies on wood thermal degradation modelling

There is substantial volume of work regarding the degradation of thermally-thick cellulosic materials by heat because of its interest in fields such as fire protection or energy conversion from biomass. Several researchers have developed numerical models of wood pyrolysis [8–22]. The most complete models describe the main transport phenomenon coupled with volumetric reactions for primary formation of tars, gases, and char. In some cases, the gas-phase cracking of tars is also included. These models describe the gas flow within the particle in conjunction with gas and solid-phase mass conservation, and total energy conservation [11,14–19]. Multiple-competing two-step reactions are used to model pyrolysis. Models for wet and dry wood pyrolysis with char shrinkage were also developed [13,15]. Detailed review on pyrolysis models has been presented [16]. Such models, after further implementations concerning heterogeneous combustion, could be incorporated in complete wildland fire spread models. Nevertheless, simplifications are required to keep computational effort within reasonable limits. Simpler models of wood pyrolysis have been developed [12,19,20]. They are based on one-step chemical kinetics to describe pyrolysis and they generally use the shrinking unreacted-core approximation which assumes that the char region is separated from virgin wood by an infinitely-thin front where pyrolysis takes place. They ignore the accumulation of gas products inside the particle assuming that volatiles escape as soon as they are formed. Moisture evaporation is generally assumed to be a thermally-controlled process which takes place across an infinitely thin front at constant temperature [19,20].

Thermal regimes which controlled the pyrolysis depend on the ratio of the external heat transfer to the internal heat transfer. This dimensionless ratio is the Biot number and can be expressed by: $Bi = hL/\lambda$ where h is an effective heat transfer coefficient, L a particle characteristic length and λ the conductivity. For inert solids, the transition between thermally-thin and thermally-thick regimes is considered to occur at Biot number equal to 0.1 [23]. The definition of the Biot number becomes more ambiguous when the particle undergoes a thermal degradation as its properties are composition- and temperature-dependent. Using a Biot number based on the conductivity of wood, Bryden et al. [17] have shown that it is appropriate to define the transition between thermally-thin and thermally-thick regimes for $Bi = 0.2$. This results in a maximum temperature difference across the particle of about 30–35 K at the transition. In agreement with Pyle and Zaror [21], Bryden et al. [17] have shown that the addition of a second dimensionless number which estimates the relative rate of external heating and pyrolysis, allows determining four regimes: thermally-thin kinetically-limited, thermally-thin heat-transfer-limited, thermally-thick and thermal wave regimes.

3. Mathematical model

The reduced model developed in this paper considers drying, pyrolysis and char oxidation processes and is based on the following assumptions.

(a) The particle loses mass via both in-depth drying and pyrolysis, and char oxidation. It loses volume only from the heterogeneous combustion at the outer surface.
(b) Vaporization is modelled by a first-order Arrhenius law [24] to avoid problems of numerical stability [22].
(c) The pyrolysis of virgin wood is modelled by a one-step reaction leading to the formation of volatiles and char, using a first-order Arrhenius law.
(d) The char-yield is constant [19,20,25,26].
(e) Char oxidation is a two-step chemical reaction.
(f) Water vapor due to the drying process and gaseous pyrolysis products are assumed in thermal equilibrium with the solid matrix.
(g) Heat and mass transfer are one-dimensional.
(h) All gaseous products escape immediately as soon as they are formed.
(i) In agreement with Grishin [24], the gaseous pyrolysis products (GPP) are an effective gas mixture of CO and CO_2.

The degradation process can be summarized by the simplified three-step mechanism:

- Endothermic drying reaction

$$\mathrm{WWF} \rightarrow \nu_{H_2O}\mathrm{H_2O} + (1-\nu_{H_2O})\mathrm{DWF} \tag{1}$$

where WWF and DWF represent moist and dry wood.
- Endothermic global pyrolysis reaction

$$\mathrm{DWF} \rightarrow \nu_{\mathrm{char}}\mathrm{Char} + (1-\nu_{\mathrm{char}})\mathrm{GPP} \tag{2}$$

- Exothermic global char oxidation reaction.

The two-step kinetic model considers a primary oxidation of carbon atoms into CO and the secondary oxidation where CO reacts with O_2 to form CO_2.

Under the previous assumptions, the balance equations for the mass of moisture, wood, and char can be written as follows:

$$\frac{\partial}{\partial t}(\rho_{\mathrm{m}}) = -R_{H_2O} \tag{3}$$

$$\frac{\partial}{\partial t}(\rho_{\mathrm{w}}) = -R_{\mathrm{pyr}} \tag{4}$$

$$\frac{\partial}{\partial t}(\rho_{\mathrm{char}}) = \nu_{\mathrm{char}} R_{\mathrm{pyr}} \tag{5}$$

where the rates of mass loss due to drying and pyrolysis are expressed from Arrhenius-type laws:

$$R_{H_2O} = \rho_{\mathrm{m}} A_{H_2O} T^{-1/2} \exp(-E_{H_2O}/\mathrm{RT}) \tag{6}$$

$$R_{\mathrm{pyr}} = \rho_{\mathrm{w}} A_{\mathrm{pyr}} \exp(-E_{\mathrm{pyr}}/\mathrm{RT}) \tag{7}$$

- During char oxidation, the rate of volume loss is given by

$$\rho_{\mathrm{char}} \frac{\partial V_{\mathrm{p}}}{\partial t} = -R_{\mathrm{char}} S_{\mathrm{p}} \tag{8}$$

If the relative velocity of air with respect to the particle is zero, the rate of reaction per external unit area can be expressed by the following correlation [27]

$$R_{\mathrm{char}} = -\frac{3}{2}\left(\frac{D_0}{2R}\right)\rho_0 \left(\frac{T}{T_0}\right)^{0.75} \frac{1}{\gamma_{\mathrm{s}}} \ln(1-\gamma_{\mathrm{s}} Y_{O_2}) \tag{9}$$

where D_0 and ρ_0 are the oxygen diffusion coefficient and the gas density at $T_0 = 273$ K, and $\gamma_{\mathrm{s}} = -0.3$ for the two-step kinetics.

If the particle is crossed by an air flow of relative velocity u, the global reaction rate R^u_{char}, can be expressed according to [28]

$$R^u_{\mathrm{char}} = R^{u=0}_{\mathrm{char}}\left(1 + 0.272 Sc^{1/3} Re_{\mathrm{p}}^{1/2}\right) \tag{10}$$

- Equation of conservation of mass flux of gaseous fuel species

$$\frac{1}{r^j}\frac{\partial}{\partial r}\left(r^j m''_{H_2O}\right) = R_{H_2O} \tag{11}$$

$$\frac{1}{r^j}\frac{\partial}{\partial r}\left(r^j m''_{\mathrm{CO}}\right) = (1-\nu_{\mathrm{char}})\alpha_{\mathrm{CO}} R_{\mathrm{pyr}} \tag{12}$$

$$\frac{1}{r^j}\frac{\partial}{\partial r}\left(r^j m''_{CO_2}\right) = (1-\nu_{\mathrm{char}})(1-\alpha_{\mathrm{CO}}) R_{\mathrm{pyr}} \tag{13}$$

where α_{CO} is the combustible part of the gaseous pyrolysis products.

- Energy balance

$$(\rho_i C_{\mathrm{p}i})_{\mathrm{s}} \frac{\partial T}{\partial t} + (m''_i C_{\mathrm{p}i})_{\mathrm{g}} \frac{\partial T}{\partial r} = \frac{1}{r^j}\frac{\partial}{\partial r}\left(r^j \lambda \frac{\partial T}{\partial r}\right) - R_{H_2O} L_{\mathrm{v}} - R_{\mathrm{pyr}} \Delta H_{\mathrm{pyr}} \tag{14}$$

with

$$(\rho_i C_{\mathrm{p}i})_{\mathrm{s}} = \rho_{\mathrm{m}} C_{\mathrm{pm}} + \rho_{\mathrm{w}} C_{\mathrm{pw}} + \rho_{\mathrm{char}} C_{\mathrm{pchar}} \tag{15}$$

$$(m''_i C_{\mathrm{p}i})_{\mathrm{g}} = m''_{H_2O} C_{\mathrm{p}H_2O} + m''_{\mathrm{CO}} C_{\mathrm{pCO}} + m''_{CO_2} C_{\mathrm{p}CO_2} \tag{16}$$

The subscript j is relative to the particle shape and is equal to 0 for slabs, 1 for cylinders and 2 for spheres. The thermal conductivity λ is assumed to vary with the composition of the solid fuel according to: $\lambda = \eta\lambda_{\mathrm{w}} + (1-\eta)\lambda_{\mathrm{char}} + \lambda_{\mathrm{m}}$, where $\eta = \rho_{\mathrm{w}}/\rho_{w_0}$ and $\lambda_{\mathrm{m}} = \chi(0.004M)$.

The initial condition is: $T(r,0) = 300$ K.

The boundary conditions are:

$$-\lambda \left.\frac{\partial T}{\partial r}\right|_{r=0} = 0 \tag{17}$$

$$-\lambda \left.\frac{\partial T}{\partial r}\right|_{r=L} = \varepsilon\left[Q_{\mathrm{ext}} - \sigma\left(T^4 - T^4_{\mathrm{amb}}\right)\right] + h_{\mathrm{conv}}(T_{\mathrm{amb}} - T) + \alpha_{\mathrm{char}} R_{\mathrm{char}} L_{\mathrm{char}} \tag{18}$$

where α_{char} is the fraction of the energy released by the char oxidation that is deposited in the particle.

The system of equations is solved by the finite volume method [29]. When char oxidation occurs, an adaptative remesh procedure is performed as the particle surface regresses.

4. Results and discussions

4.1. Model validation

The pyrolysis model is validated against the experiments of Galgano and Di Blasi [19]. They considered wood cylinders of radius 0.02 m submitted to an external heat flux of 49 kW m^{-2}.

Table 1
Fuel property values and thermokinetic constants

Property	Wood	Douglas Pine [24]
ρ_w (kg m^{-3})	650 [19]	710
ρ_{char} (kg m^{-3})	147 [19]	180
ΔH_{pyr} (kJ kg^{-1})	430 [19]	418
L_{char} (kJ kg^{-1})		-1.2×10^4
C_{pw} (kJ kg^{-1} K^{-1})	1.5 [19]	1.46
C_{pc} (kJ kg^{-1} K^{-1})	2.1 [19]	1.1
λ_w (W m^{-1} K^{-1})	0.3 [19]	0.24
λ_c (W m^{-1} K^{-1})	0.25 (best fit)	0.1
ε_w	0.9 [30]	0.9
A_{H_2O} (s^{-1} K$^{-1/2}$)	6×10^5 [24]	6×10^5
A_{pyr} (s^{-1})	3.5×10^{10} [31]	3.64×10^4
E_{H_2O} (kJ mol^{-1})	48.22 [24]	48.22
E_{pyr} (kJ mol^{-1})	137 [31]	60.27

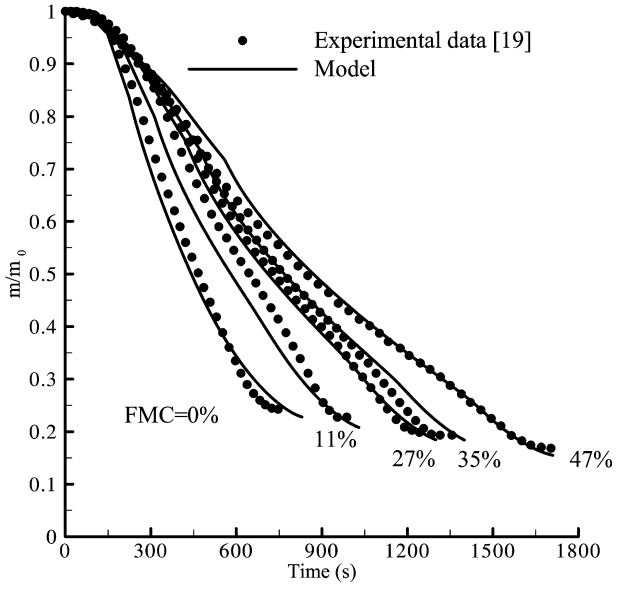

Fig. 1. Time evolution of the solid mass fraction for different values of FMC. Experimental results reported in [19] are also shown.

Fuel properties and thermokinetic constants used for the predictions are summarized in Table 1. The biggest uncertainty is related to the coefficients of the pyrolysis model given in the literature. The values of the pre-exponential factor and the activation energy adopted are close to those used by Di Blasi for cellulose [31].

Fig. 1 represents the time evolution of the normalized mass of the particle. Since experiments were carried out in a non-oxidizing medium, char oxidation cannot occur. Model results present a quite good agreement with experiments whatever the FMC considered.

4.2. Thermal regime for wildland fuel pyrolysis

The model is applied to cellulosic materials representative of the Mediterranean biomass in order to assess the validity of the thermally-thin pyrolysis assumption currently used in wildland fire models. During wildfire spread, pyrolysis products mix and react with available oxygen to generate the flame. Consequently, oxygen is highly consumed by homogeneous combustion and thus a small amount of oxygen mass fraction diffuses towards the solid surface, which limits char oxidation. This means that pyrolysis and char oxidation processes occur successively. Char oxidation can then be disregarded as it does not influence pyrolysis process. Particles are submitted to radiant heat fluxes ranging from 10 to 150 kW m^{-2}. Particle characteristic lengths in the range 0.05–3 mm and FMC in the range 0–100% are considered. Spheres, cylinders and slabs are considered. Douglas pine is used as fuel. Thermal properties values and thermokinetic constants of this fuel are listed in Table 1. The transition between thermally-thin and thermally-thick pyrolysis regimes can be determined by a threshold value on the Biot number defined by:

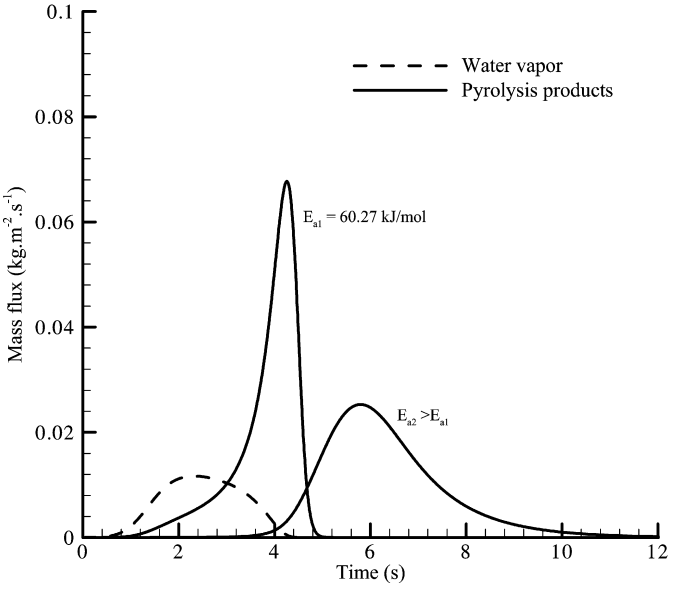

Fig. 2. Time evolution of the vapor and pyrolysis mass flow rates for a thermally-thin 0.25 mm-radius sphere and FMC = 30% exposed to a radiant heat flux of 40 kW m^{-2}.

$$Bi = \frac{\varepsilon Q_{ext} L}{\lambda \Delta T} \tag{19}$$

L is a characteristic length depending on the particle geometry while ΔT refers to the difference between a characteristic pyrolysis temperature and the ambient. During thermal degradation, both emissivity and conductivity may vary significantly leading to an unclear definition of the Biot number. Bryden et al. [17] argued that the limiting Biot number for thermally-thin regime occurs after the wood is dried and consequently the particle size limit for thermally-thin pyrolysis is independent on FMC. This assertion is strictly valid if drying and pyrolysis occurs successively in the thermally-thin regime. For wood species typical of Mediterranean ecosystems, the onset of pyrolysis occurs at low temperature which explains the low activation energy of pyrolysis (Table 1). Fig. 2 shows both vapor and pyrolysis mass flow rates as a function of time for a sphere of radius 0.25 mm and FMC of 30% submitted to a 40 kW m^{-2} radiant heat flux. Since, the maximum temperature difference across the particle during wood degradation process is less than 20 K, it is considered that pyrolysis occurs in the thermally-

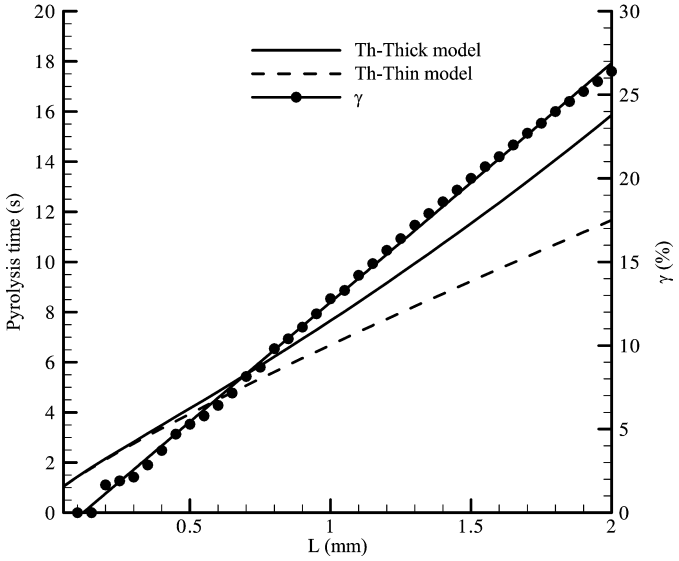

Fig. 3. Evolution of the pyrolysis times obtained from thermally-thin and thermally-thick models and γ as a function of the characteristic length for dry cylinders. The radiant heat flux is 40 kW m^{-2}.

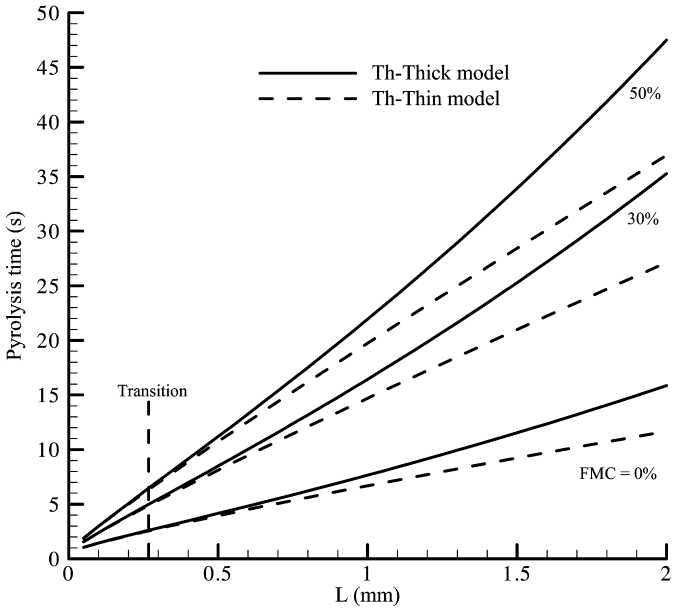

Fig. 4. Pyrolysis times as a function of the radius of a cylinder for different FMC. The radius at which transition between thermally-thin and thermally-thick pyrolysis occurs is indicated. The radiant heat flux is 40 kW m^{-2}.

thin regime in agreement with Bryden et al. [17]. Results reveal that although the particle is thermally-thin, drying and pyrolysis processes overlap. These two processes become successive for higher pyrolysis activation energies. This overlapping explains the difficulty to initiate flaming combustion for thin and wet vegetal particles as water vapor dilutes pyrolysis products. Consequently, the initial FMC may affect the transition between thermally-thin and thermally-thick pyrolysis regimes. This will be studied below.

In order to define an adequate Biot number, a criterion has to be defined to delimit thermal regimes for pyrolysis. For wildland fires, the flaming residence time is directly related to the pyrolysis time. Consequently, in order to evaluate the transition regime, the relative variation between pyrolysis times determined for both regimes is considered:

$$\gamma = 100 \times \left(\frac{t_{\mathrm{p,thick}} - t_{\mathrm{p,thin}}}{t_{\mathrm{p,thick}}} \right) \tag{20}$$

Fig. 3 shows the evolution of pyrolysis times obtained from both thermally-thin and thermally-thick models and γ versus the particle radius for cylindrical dry particles exposed to a radiant heat flux of 40 kW m^{-2}. For small particle radius, both models provide the same solution. As the radius increases, the relative discrepancy between the two models increases as the thermally-thin assumption becomes no longer valid. The regime transition may be defined by a 2% threshold value on γ. A slight change in this threshold value does not modify significantly the particle size limit in the thermally-thin regime. A 2%-threshold value on γ results in a maximum temperature difference across the particle during pyrolysis less than 20 K.

In order to study the effect of FMC on the transition, the evolution of pyrolysis times obtained from both thermally-thin and thermally-thick models as a function of the particle characteristic length for FMC of 0, 30 and 50% is shown in Fig. 4. Cylinders submitted to an external radiant heat flux of 40 kW m^{-2}, are considered. It is worthy noting that the same conclusions can be drawn independently of the particle shape and the external heat flux. As shown previously, vapor and pyrolysis mass flow rates overlap even in the thermally-thin regime due to the low pyrolysis activation energy (Table 1). This explains that, for given external heat flux and particle size, the pyrolysis time increases with FMC whatever the thermal regime. For higher pyrolysis activation energies, drying and pyrolysis processes would become successive in the thermally-thin regime and FMC would not affect the pyrolysis time [19]. Although pyrolysis time increases with FMC in the thermally-thin pyrolysis regime, Fig. 4 shows that FMC has not a significant effect on the transition radius. The critical radius is 0.265, 0.27 and 0.26 mm for FMC of 0, 30, and 50%, respectively. Since the size transition delimiting thermally-thin and thermally-thick pyrolysis is nearly independent of FMC, the Biot number can be defined as:

$$Bi = \frac{\varepsilon_{\mathrm{w}} Q_{\mathrm{ext}} L}{\lambda_{\mathrm{w}} \Delta T} \tag{21}$$

The characteristic length L is the half of the slab thickness. It corresponds to the radius for both cylinder and sphere. The effects of the particle shape on the regime transition can be deduced from the following analysis. Let us consider a dry particle. In the thermally-thin pyrolysis regime the integration of Eqs. (12)–(14) over the whole particle volume leads to:

$$m_i'' S_{\mathrm{p}} = (1 - \nu_{\mathrm{char}}) \alpha_i R_{\mathrm{pyr}} V_{\mathrm{p}}, \quad i = \mathrm{CO}, \mathrm{CO_2} \tag{22}$$

$$\rho C_{\mathrm{p}} \frac{\partial T}{\partial t} V_{\mathrm{p}} = \left\{ \varepsilon \left[Q_{\mathrm{ext}} - \sigma \left(T^4 - T_{\mathrm{amb}}^4 \right) \right] + h_{\mathrm{conv}} (T_{\mathrm{amb}} - T) \right\} S_{\mathrm{p}} - R_{\mathrm{pyr}} \Delta H_{\mathrm{pyr}} V_{\mathrm{p}} \tag{23}$$

These two equations have to be solved in connection with Eqs. (3) and (4).

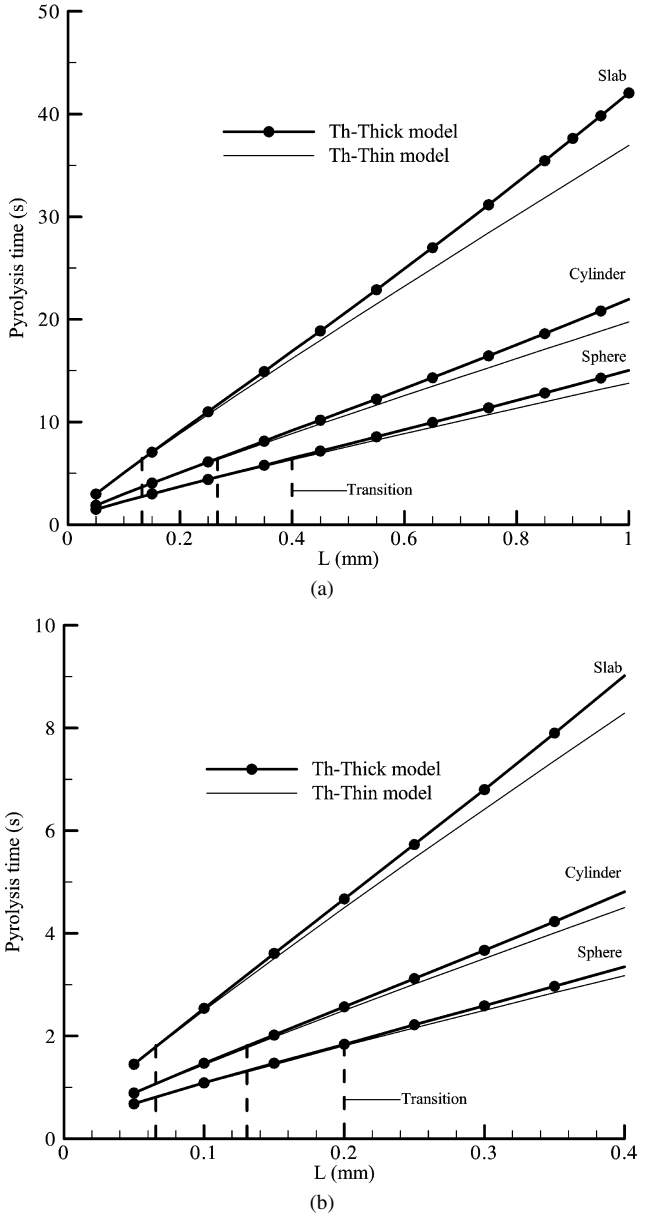

Fig. 5. Pyrolysis time as a function of the particle radius for an external heat flux of (a) 40 kW m^{-2} and (b) 80 kW m^{-2}. Slabs, cylinders and spheres are considered.

A dimensional analysis shows that the last term on the right-hand side of Eq. (23) can be neglected due the low heat of pyrolysis emphasizing that the effect of the particle shape is related only to the particle surface-area-to-volume ratio, $\sigma_p = S_p/V_p$. As transition occurs for a critical value of σ_p whatever the particle geometry, the corresponding particle characteristic lengths are related by

$$L_{cr,slab} = L_{cr,cylinder}/2 = L_{cr,sphere}/3 \quad (24)$$

This behavior appears clearly by comparing the evolutions of the pyrolysis time versus the particle characteristic length for external heat fluxes of 40 and 80 kW m^{-2}. For an incident flux of 40 kW m^{-2} (Fig. 5(a)), transition occurs for a characteristic length of 0.13 mm for a slab, whereas it is 0.26 mm for a cylinder and 0.4 mm for a sphere. When the external heat flux is

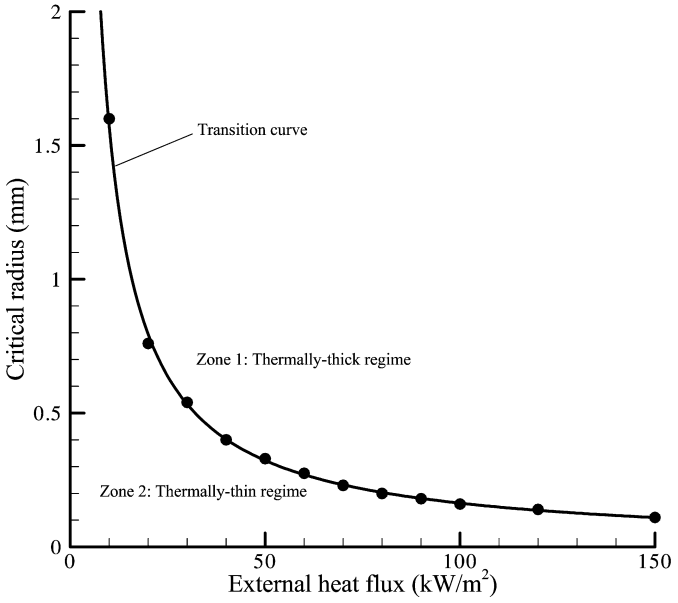

Fig. 6. Evolution of the transition radius as a function of the external radiant heat flux for spheres.

increased to 80 kW m^{-2} (Fig. 5(b)), L_{cr} is equal to 0.065, 0.13 and 0.20 mm, respectively. These values satisfy Eq. (24).

Using a characteristic pyrolysis temperature of 500 K [2], the transition Biot number (Eq. (21)) is found to be 0.1, 0.2 and 0.3 for a slab, a cylinder and a sphere, respectively. Eq. (24) suggests that a Biot number independent of the particle geometry can be defined as:

$$Bi = \frac{\varepsilon_w Q_{ext}}{\lambda_w \sigma_p \Delta T} \quad (25)$$

Using this definition of the Biot number, the transition between thermally-thin and thermally-thick pyrolysis occurs at $Bi = 0.1$ whatever the geometry considered.

Fig. 6 shows the evolution of the transition radius as a function of the external radiant heat flux for a sphere. As shown previously, the transition characteristic length for cylinder and slab can be deduced from Eq. (24) and the above-drawn conclusions remain valid for cylinder and slab. It is found that the transition radius decreases with increasing radiant flux. This curve allows distinguishing thermally-thin and thermally-thick pyrolysis regimes. Particles of 0.5 mm radius are thermally thin for a flux less than 30 kW m^{-2} and become thermally thick beyond. For wildland fire applications where the fuel particles are often exposed to strong radiant heat fluxes, the range of validity of the thermally-thin pyrolysis assumption is then very limited. It must be underlined that even thin particles such as pine needles have likely to be treated as thermally thick for typical fires in Mediterranean landscapes.

4.3. Further discussions

Since pyrolysis of fuel particles in wildland fire spread occurs in the thermally-thick regime, it is important to know which mechanism controls the pyrolysis process. The characteristic times for heat diffusion and kinetics are given by $\tau_d =$

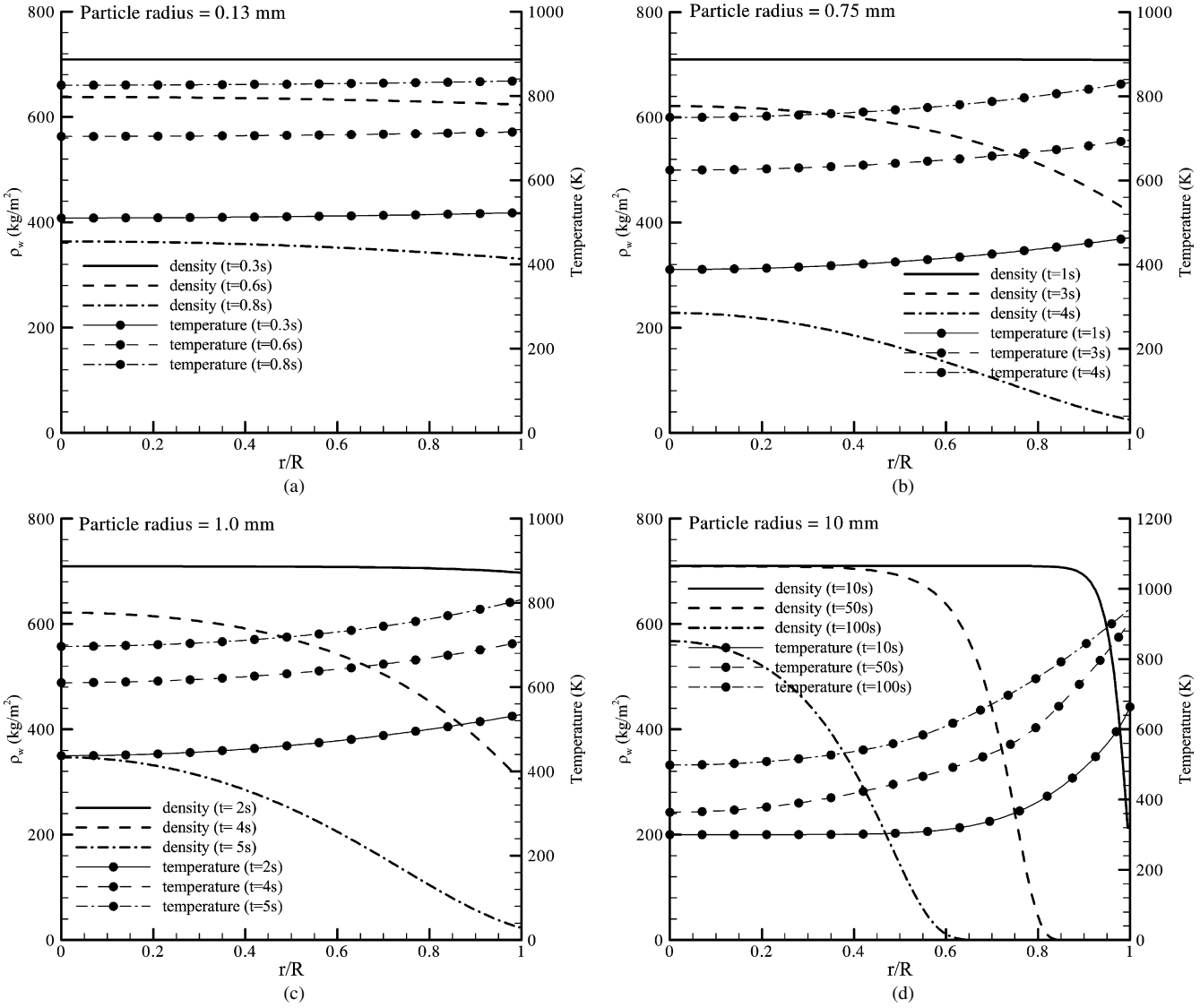

Fig. 7. Temperature and wood density profiles across cylindrical particles submitted to an external radiant flux of 80 kW m^{-2} at different times and for particle radii of: (a) 0.13 mm, (b) 0.75 mm, (c) 1 mm, and (d) 10 mm.

$L^2/\alpha_{\mathrm{th,d}}$ and $\tau_c = (A_{\mathrm{pyr}}\, e^{-\frac{E_{\mathrm{pyr}}}{RT}})^{-1}$ where $\alpha_{\mathrm{th,d}} = \lambda_w/(\rho_w C_{\mathrm{pw}})$ is the thermal diffusivity. Two limiting cases can be distinguished: a kinetically-controlled regime for $\tau_d \ll \tau_c$ and a heat-diffusion-controlled regime for $\tau_d \gg \tau_c$. For the latter, the chemical process is fast and the pyrolysis front can be represented as an infinitely thin front. This is the starting point of the shrinking unreacted-core model.

Fig. 7 shows temperature and wood density profiles across cylindrical particles at different times for an external heat flux of 80 kW m^{-2} and different particle radius. For the smallest particles (the value of 0.13 mm corresponds to the transition radius), these profiles are almost flat with the exception of a slight temperature gradient which takes place inside the particle near the outer surface. In this case $\tau_c \approx 0$ and the pyrolysis process is kinetically-controlled. As the particle size increases, the penetration of the thermal wave is no longer infinitely fast and temperatures profiles exhibit more variation across the particle (Figs. 7(b) and 7(c)). As a consequence, wood density increases as the distance from the particle center decreases. However, pyrolysis occurs in the major part of the particle which suggests that for particles of 0.75 and 1 mm radius, pyrolysis is kinetically-controlled. For larger particles, as the particle size increases, the wood density profiles show a sharp variation which suggests that the process becomes controlled by heat diffusion (Fig. 7(d)). Although not shown in the figures, both pyrolysis and evaporation times exhibit a linear increase with FMC as reported in previous experimental and theoretical analysis [12,19].

4.4. Application to firebrand combustion

In this section the model is applied to describe the combustion of firebrands. Experimental data of the Northern Forest Fire Laboratory, reported by Muraszew et al. [32] are used for comparisons. These experiments consider the combustion of oven dry 12.7 cm-long cylinders, wind relative velocities of 4.47

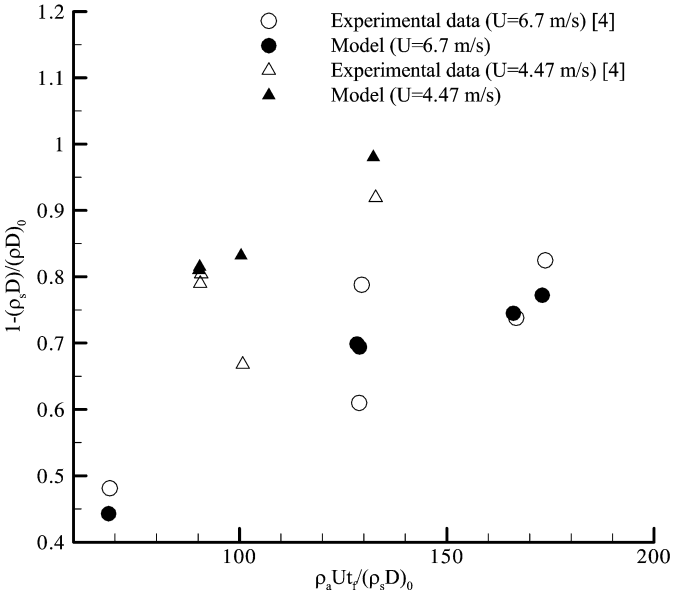

Fig. 8. Fractional loss of density × thickness as a function of a regression variable for Ponderosa Pine firebrands.

and 6.70 m s^{-1} and different initial particle sizes and masses. Wood material is pyrolyzed by heat supplied from homogeneous combustion at the outer surface. Consequently, during the pyrolysis process, the surface particle temperature remains constant and equals to 993 K [33]. The properties of air surrounding the particle are evaluated at average conditions which are taken to be the ambient pressure and the arithmetic mean of the surface particle temperature and the ambient temperature. Fig. 8 shows the evolution of the ratio $(\rho_s D)/(\rho_s D)_0$ as a function of $(\rho_a U t_f)/(\rho_s D)_0$ where ρ_s, D, U, t_f and ρ_a represent the solid density, the particle diameter, the wind velocity, the final test time, and the air density, respectively. The subscript 0 denotes initial values. These two dimensionless groups are taken from the analysis of Albini [4] based on the data of Muraszew et al. [32]. The data concerns Ponderosa Pine. Fig. 8 shows that the agreement between the model results and the experimental data is good with a maximum in deviation of 20%.

5. Conclusion

A simplified thermally-thick wildland fuel degradation model is developed. Model results are found in agreement with experimental data. The model is applied to assess the validity of the thermally-thin pyrolysis assumption currently used in wildland fire behavior models. The following conclusions can be drawn:

- For a given radiant flux, FMC does not affect the particle size limit for thermally-thin pyrolysis. For the present purpose, this result is not direct since drying and pyrolysis overlaps even in the thermally thin regime due to the low activation energy of pyrolysis.
- Geometry has a significant effect on the particle size limit for thermally-thin pyrolysis. For a given flux, results reveal that the transition between the thermally-thin and the thermally-thick regimes occurs for the same value of the particle surface-to-volume ratio which leads to the determination of the corresponding characteristic lengths for slabs, spheres, and cylinders.
- Defining the Biot number as $Bi = \frac{\varepsilon_w Q_{ext}}{\lambda_w \sigma_p \Delta T}$, transition occurs when $Bi = 0.1$ whatever the particle shape.
- The range of validity of the thermally-thin pyrolysis assumption in wildland fire behavior modelling is all the more limited as the heat transfer from the flame to the unburnt fuel bed is high. The characteristic length for which transition occurs is determined as a function of the overhead flame radiative heat flux.
- Results suggest that pyrolysis is kinetically-controlled for fine particles that are responsible for fire spread. As particle size increases, the characteristic time of heat diffusion becomes smaller and the pyrolysis becomes progressively controlled by heat diffusion. For low characteristic diffusion time, the pyrolysis front can be approximated by an infinitely thin front separating char layer from virgin wood.

Finally, comparisons with experiments show that the model is relevant to describe firebrand combustion.

References

[1] N.D. Burrows, Flame residence times and rates of weigh loss of eucalypt forest fuel particles, Int. J. Wildland Fire 10 (2) (2001) 137–143.
[2] B. Porterie, D. Morvan, L.C. Loraud, M. Larini, Firespread through fuel beds—modelling of wind-aided fires and induced hydrodynamics, Phys. Fluids 12 (2000) 1762–1782.
[3] B. Porterie, J.C. Loraud, L.O. Bellemare, J.L. Consalvi, A physically-based model of the onset of crowning, Combust. Sci. Technol. 175 (2003) 1109–1141.
[4] F.A. Albini, Spot fire distance from burning trees—a predictive model, Gen. Tech. Rep. INT-56, USDA Forest Service, Ogden, Utah, 1979.
[5] G.M. Byram, K.P. Davis, W.R. Krumm, Forest Fire: Control and Use, McGraw–Hill, New York, 1959.
[6] A.L. Berlad, S.L. Lee, Long-range spotting, Combust. Flame 12 (1968) 172–174.
[7] A. Muraszew, J.B. Fedele, Statistical model for spot fire hazard, Aerospace Rep. ATR-77(7588)-1, The Aerospace Corp., El Segundo, CA, 1976.
[8] D.L. Simms, Damage to cellulosic solids by thermal radiation, Combust. Flame 6 (1962) 303–318.
[9] A.F. Roberts, A review of kinetics data for the pyrolysis of wood and related substances, Combust. Flame 14 (1970) 261–272.
[10] M.A. Kanury, Thermal decomposition kinetics of wood pyrolysis, Combust. Flame 18 (1972) 75–83.
[11] S.S. Alves, J.L. Figueiredo, A model for pyrolysis of wet wood, Chem. Engrg. Sci. 44 (1989) 2861–2869.
[12] J. Saastamoinen, J.R. Richard, Simultaneous drying and pyrolysis of solid fuel particles, Combust. Flame 106 (1996) 288–300.
[13] C. Di Blasi, Heat, momentum, and mass transport through a shrinking biomass particle exposed to thermal radiation, Chem. Engrg. Sci. 51 (1996) 1121–1132.
[14] K.W. Ragland, J.C. Boerger, A.J. Baker, A model of chunk wood combustion, Forest Products J. 38 (2) (1988) 27–32.
[15] W.R. Chan, M. Kelbon, B.B. Krieger, Modelling and experimental verification of physical and chemical processes during pyrolysis of large biomass particle fuel, Fuel 64 (1985) 1505–1513.
[16] C. Di Blasi, Modelling and simulation of combustion processes of charring and non-charring solid fuels, Prog. Energy Combust. Sci. 19 (1993) 71–104.
[17] K.M. Bryden, K.W. Ragland, C.J. Rutland, Modelling thermally-thick pyrolysis of wood, Biomass Bioenergy 22 (2002) 41–53.

[18] A. Atreya, Pyrolysis, ignition and fire spread on horizontal surface of wood, National Bureau of Standards, Rep. NBS-GCR-83-449, 1984.
[19] A. Galgano, C. Di Blasi, Modelling the propagation of drying and decomposition fronts in wood, Combust. Flame 139 (2004) 16–27.
[20] M.J. Spearpoint, J.G. Quintiere, Predicting the burning of wood using an integral model, Combust. Flame 123 (2000) 308–324.
[21] D.L. Pyle, C.A. Zaror, Heat transfer and kinetics in the low temperature pyrolysis of solids, Chem. Engrg. Sci. 39 (1984) 147–158.
[22] H. Thunman, B. Leckner, F. Niklasson, F. Johnsson, Combustion of wood particles—a particle model for Eulerian calculations, Combust. Flame 129 (2002) 30–46.
[23] J.F. Sacadura, Initiation aux transferts thermiques, Techn. Doc., Lavoisier, Paris, 1982.
[24] A.M. Grishin, in: F.A. Albini (Ed.), Mathematical Modelling of Forest Fires and New Methods of Fighting Them, Pub. House Tomsk University, Tomsk, Russia, 1997.
[25] C. Di Blasi, E. Gonzalez Hernandez, A. Santoro, Radiative pyrolysis of single moist wood particles, Indust. Engrg. Chem. Res. 39 (2000) 873–882.
[26] C. Di Blasi, C. Branca, C. Santoro, E. Gonzalez Hernandez, Pyrolytic behaviour and products of some wood varieties, Combust. Flame 124 (2001) 165–177.
[27] M.F.R. Mulcahy, I.W. Smith, Kinetics of combustion of pulverized fuels: a review of theory and experiment, Rev. Pure Appl. Chem. 19 (1969) 81–106.
[28] N. Frössling, Über die verunstung fallender tropfen, Gerlands Beitr. Geophys. 52 (1938) 170–216.
[29] S.V. Patankar, Numerical Heat Transfer and Fluid Flow, McGraw–Hill, London, 1980.
[30] W.J. Parker, Prediction of the heat release rate of Douglas Fir, in: Proceedings of the 2nd Int. Symp. Fire Safety Science, 1989, pp. 337–346.
[31] C. Di Blasi, Processes of flames spreading over the surface of charring fuels: effects of the solid thickness, Combust. Flame 97 (1994) 225–239.
[32] A. Muraszew, J.B. Fedele, W.C. Kuby, Firebrand investigation, Aerospace Rep. ATR-75(7470)-1, The Aerospace Corp., El Segundo, CA, 1975.
[33] S.D. Tse, A.C. Fernandez-Pello, On the flight paths of metal particles and embers generated by power lines in high winds—a potential source of wildland fires, Fire Safety J. 30 (1998) 333–356.